

## Rapid Communications

The Rapid Communications section is intended for the accelerated publication of important new results. Manuscripts submitted to this section are given priority in handling in the editorial office and in production. A Rapid Communication may be no longer than 3½ printed pages and must be accompanied by an abstract. Page proofs are sent to authors, but, because of the rapid publication schedule, publication is not delayed for receipt of corrections unless requested by the author.

Observation of the decay of a new isotope  $^{57}\text{Cu}$  and its mirror transition

T. Shinozuka and M. Fujioka

Cyclotron and Radioisotope Center, Tohoku University, Sendai 980, Japan

H. Miyatake, M. Yoshii, H. Hama, and T. Kamiya

Department of Physics, Tohoku University, Sendai 980, Japan

(Received 30 July 1984)

The decay of  $^{57}\text{Cu}_{28}$  produced with the  $^{58}\text{Ni}(p,2n)$  reaction was identified by a 1112-keV  $\gamma$  ray occurring in its daughter nucleus  $^{57}\text{Ni}$  and the half-life and  $\beta^+$  end-point energy were measured to be  $223 \pm 16$  ms and  $7720 \pm 130$  keV, respectively, applying a technique of fast transportation of irradiated targets. The  $\log ft$  value and Gamow-Teller matrix element of the ground-to-ground mirror transition of  $^{57}\text{Cu}_{28}$  ( $T_z = -\frac{1}{2}$ )  $\rightarrow$   $^{57}\text{Ni}_{29}$  ( $T_z = \frac{1}{2}$ ) was deduced to be  $\log ft = 3.71 \pm 0.05$  and  $\langle \sigma \tau \rangle = 0.37 \pm 0.11$ . The present results indicate a large reduction of  $\langle \sigma \tau \rangle$  from the single particle value (1.291) although  $^{57}\text{Cu}$  is a nucleus obtained by adding one proton to the  $^{56}\text{Ni}_{28}$  core.

The superallowed  $\beta$  decay connecting the two ground states of  $T_z = \pm \frac{1}{2}$  mirror nuclei can be described in terms of both Fermi and Gamow-Teller (GT) transitions. While the Fermi part of the transition strength is approximately constant because of the approximate conservation of isospin together with the exact conservation of vector current, the GT part should depend strongly on the nuclear wave functions as well as the effects outside the conventional nuclear structure, i.e., the so called renormalization effect<sup>1</sup> on the axial vector coupling constant  $g_A$ . Moreover, the small deviation from constancy of the Fermi strength can be estimated<sup>2</sup> accurately enough to single out reliably the contribution of the GT part from the experimental  $\beta$  strength of a  $T = \frac{1}{2}$  mirror transition. Therefore, the measurement of the  $\beta$  strength between mirror nuclei, on the one hand, offers a good means for testing the nuclear shell model provided the renormalized coupling constant  $g_A^{\text{eff}}$  is taken from systematics, or, on the other hand, for extracting the renormalization effect itself provided the shell model wave functions can be reliably calculated.

In this paper we report on the decay characteristics of a new mirror nucleus  $^{57}\text{Cu}_{28}$ , which is interesting and important because it is a nucleus consisting of the  $^{56}\text{Ni}$  core and one proton in the  $p_{3/2}$  shell. The observation of mirror nuclei in the  $f_{7/2}p_{3/2}$  shell region are especially difficult because of their short half-lives and small production cross sections, which are the common features of nuclei far from the  $\beta$ -stability line. In order to study such nuclei we have developed a high-speed target-rotation device<sup>3</sup> (TARO), by means of which targets can be brought to a low-background area in 60 ms after irradiation.

The  $^{57}\text{Cu}$  nuclei were produced via the  $^{58}\text{Ni}(p,2n)^{57}\text{Cu}$  reaction with 23–34 MeV proton beams of 0.2–0.3  $\mu\text{A}$  in-

tensities from the cyclotron of Tohoku University. The TARO consists of a thin rotating plate with targets and a stepping motor both in a vacuum chamber; it has high position accuracy and high slewing pulse rate (see Fig. 1). To reduce the accumulation of long-lived activities, 16  $^{58}\text{Ni}$  targets ( $\sim 3$  mg/cm<sup>2</sup>, 99.76% enriched) were mounted on the rotating plate. A target was irradiated by the pulsed proton beam for 0.2 s, transferred to the shielded detector region in 0.06 s, and the counting system was opened for 1.28 s. To reduce the effects of long-lived activities it was also important to optimize the order of irradiation of the 16 targets, and to avoid the neutron-induced background and  $\gamma$  flash during the counting period it was essential to use the beam pulsing.

The  $\gamma$ -ray spectrum was measured with a 96 cm<sup>3</sup> Ge(HP) detector behind a 5-mm-thick copper plate for stopping posi-

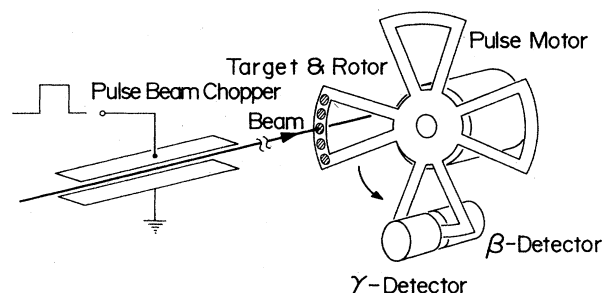


FIG. 1. Schematic drawing of the high-speed target rotation device (TARO). Target rotation, cyclotron-beam chopping, and counting of  $\beta$  and  $\gamma$  rays are sequentially controlled by a microcomputer.

trons. The  $\beta^+$ -ray spectrum was measured with a planar Ge(HP) detector of  $490\text{ mm}^2 \times 10\text{ mm}$  behind a  $6.87\text{-mg/cm}^2$  Mylar window at the detector position of TARO and a  $127\text{-}\mu\text{m}$  Be window of the detector. The total energy loss of positrons in these foils was estimated to be  $51\text{ keV}$  at  $E_{\beta^+} = 7\text{ MeV}$ . These spectra were measured by the method of multispectra using an on-line data processing system.

In the  $\gamma$ -ray energy spectrum we discovered a  $\gamma$ -ray decaying with a half-life of  $T_{1/2} = 233 \pm 16\text{ ms}$ , which we assigned as depopulating the  $1112\text{-keV}$  second-excited state<sup>4</sup> ( $J^\pi = \frac{1}{2}^-$ ) of  $^{57}\text{Ni}$  fed from the decay of  $^{57}\text{Cu}$ ; we determined the  $\gamma$ -ray energy as  $1111.7 \pm 0.5\text{ keV}$ . Figure 2 shows a  $\gamma$ -ray spectrum and the decay of the  $1111.7\text{-keV}$   $\gamma$ -ray intensity. This value of half-life is compatible with a value of  $0.2\text{ s}$  predicted from the gross theory of  $\beta$  decay.<sup>5</sup> Furthermore, the excitation functions of  $^{58}\text{Ni}(p,n)^{58}\text{Cu}$ ,  $^{58}\text{Ni}(p,2n)^{57}\text{Cu}$  and  $^{58}\text{Ni}(p,\alpha n)^{54m}\text{Co}$  were obtained from the yield curves of the corresponding  $\gamma$  rays ( $E_p = 23\text{--}34\text{ MeV}$ ), and compared with the theoretical cross sections calculated by the ALICE code taking into account the precompound process.<sup>6</sup> The experimental excitation function from the  $1111.7\text{-keV}$   $\gamma$ -ray agreed best with the theoretical one for  $^{58}\text{Ni}(p,2n)^{57}\text{Cu}$ , supporting the identification of  $^{57}\text{Cu}$ . We found no other  $\gamma$  rays following the decay of  $^{57}\text{Cu}$ .

The  $\beta^+$ -ray spectrum of  $^{57}\text{Cu}$  was interfered by the  $\beta^+$  rays from  $^{54g}\text{Co}(T_{1/2} = 193\text{ ms}, E_{\beta^+}^{\text{max}} = 7.3\text{ MeV})$ <sup>4</sup> and  $^{58}\text{Cu}(3.2\text{ s}, 7.5\text{ MeV})$ <sup>4</sup> having end-point energies close to the value predicted<sup>7</sup> for  $^{57}\text{Cu}$ . We could, however, determine the  $E_{\beta^+}^{\text{max}}$  of  $^{57}\text{Cu}$  using a "time-filtering" analysis of the time dependence of the measured  $\beta^+$  ray spectrum as shown in Fig. 3. The time-filtered  $\beta^+$ -ray spectrum (II B) corresponding to the component of shorter half-life should consist of the  $\beta^+$  rays from  $^{57}\text{Cu}$  and  $^{54g}\text{Co}$ . Since this spectrum showed a  $\beta^+$ -ray end-point energy larger than  $E_{\beta^+}^{\text{max}}(^{54g}\text{Co})$  obtained by the  $^{54}\text{Fe}(p,n)^{54}\text{Co}$  reaction, we derived  $E_{\beta^+}^{\text{max}}(^{57}\text{Cu})$  by a Kurie-plot analysis of that part of

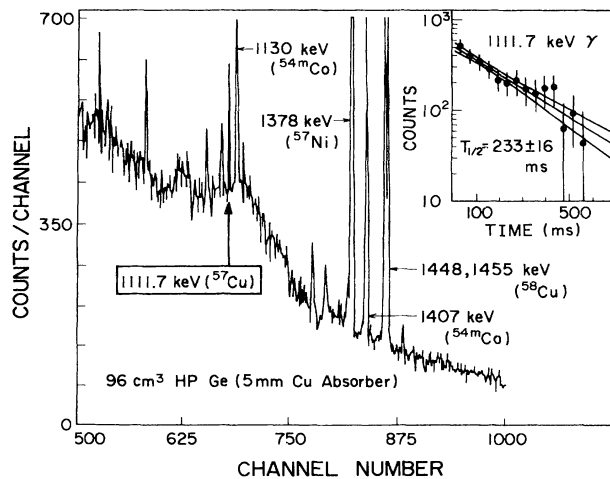


FIG. 2.  $\gamma$ -ray spectrum obtained by a  $30\text{-MeV}$  proton bombardment of  $^{58}\text{Ni}$  targets. Nuclei  $^{54m}\text{Co}$ ,  $^{57}\text{Ni}$ ,  $^{58}\text{Cu}$ , and  $^{57}\text{Cu}$  are produced via  $^{58}\text{Ni}(p,\alpha n)$ ,  $(p,pn)$ ,  $(p,n)$ , and  $(p,2n)$  reactions, respectively. The inset shows a decay curve of the  $1111.7\text{-keV}$   $\gamma$ -ray accumulated in a series of  $200\text{-ms}$  irradiations and  $1.28\text{-s}$  countings. The  $\gamma$ -ray counts are obtained by the spectrum analysis code SAMPO.

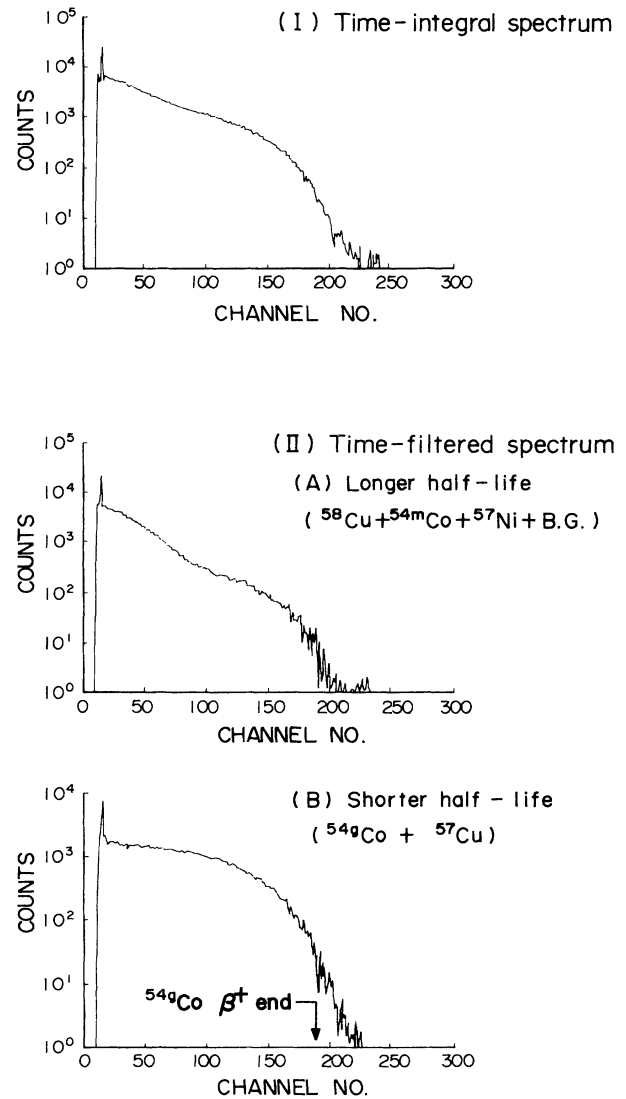


FIG. 3. Time-integral (I) and time-filtered  $\beta^+$  spectra (II A) and (II B). The energy ( $E_{\beta^+}$ ) and time ( $t_{\beta^+}$ ) of  $\beta^+$  rays are stored as multispectra, from which time-filtered spectra, (II A) and (II B), are constructed by a decay analysis of every energy channel; two time components,  $T_{1/2}^{\text{long}} = \infty$  and  $T_{1/2}^{\text{short}} = 0.2\text{ s}$  are used in this analysis. The time-filtered spectrum of longer half-life (A) should be composed of  $\beta^+$  ray from the decay of  $^{58}\text{Cu}(T_{1/2} = 3.2\text{ s})$ ,  $^{54m}\text{Co}(1.24\text{ m})$ ,  $^{57}\text{Ni}(36\text{ h})$ , etc., while that of shorter half-life (B) from the decay of  $^{54g}\text{Co}(193\text{ ms})$  and  $^{57}\text{Cu}(233\text{ ms})$ .

the spectrum having  $E_{\beta^+} > E_{\beta^+}^{\text{max}}(^{54g}\text{Co})$  in the time-filtered spectrum. In this analysis we followed the method of Rehfeld *et al.*;<sup>8</sup> we also assumed a semiempirical detector response function determined in Ref. 9. Thus, we obtained  $E_{\beta^+}^{\text{max}}(^{57}\text{Cu}) = 7.72 \pm 0.13\text{ MeV}$ . This end-point energy agrees well with the value estimated using the semiempirical formula of Jänecke<sup>10</sup> for Coulomb displacement energies. The branching ratio to the  $1111.7\text{-keV}$  excited state of  $^{57}\text{Ni}$  was obtained to be  $3.7 \pm 1.7\%$  from simultaneously measured  $\beta$ - and  $\gamma$ -ray spectra. Table I summarizes the  $\log ft$  values and GT matrix elements for the decay of  $^{57}\text{Cu}$  to the

TABLE I.  $\log ft$  values and GT matrix elements for the  $\beta^+$  decay of  $^{57}\text{Cu}$  to  $^{57}\text{Ni}$ .

$E_f$ (keV)	$J_f^{\pi f}$	$\log ft^a$	$\langle\sigma\tau\rangle_{\text{expt}}$	$\langle\sigma\tau\rangle_{\text{sp}}$
0	$\frac{3}{2}^-$	$3.71 \pm 0.05$	$0.37 \pm 0.11$	1.231
1111.7	$\frac{1}{2}^-$	$4.80 \pm 0.24$	$0.25 \pm 0.06$	1.155

<sup>a</sup>The  $f$  values calculated according to Ref. 11 are  $21069 \pm 1673$  and  $10141 \pm 933$  for the ground and 1111.7-keV levels of  $^{57}\text{Ni}$ , respectively.

ground and second-excited (1111.7-keV) states of  $^{57}\text{Ni}$ . The  $\log ft$  value of 3.7 for the ground transition indicates a superallowed transition, which establishes the spin-parity assignment of  $\frac{3}{2}^-$  to  $^{57}\text{Cu}$  (ground state), in agreement with the shell model expectation. This assignment is consistent with  $\log ft = 4.80$  indicating an allowed transition to the 1111.7-keV  $\frac{1}{2}^-$  state of  $^{57}\text{Ni}$ . In deriving  $\langle\sigma\tau\rangle_{\text{expt}}$  the formulae of Ref. 2 were used. We note a large reduction of GT matrix elements in comparison with the single particle values. Since the last proton in  $^{57}\text{Cu}$  cannot be excited singly by the residual interaction, the large reduction of  $\langle\sigma\tau\rangle$  should reflect directly the effect of excitation of the  $^{56}\text{Ni}$  core; for a similar reduction of the magnetic moment of  $^{57}\text{Ni}$  (ground state) due to the core excitation, see Ref. 12.

In the region of  $sd$ -shell nuclei a rather complete analysis<sup>13</sup> of  $\langle\sigma\tau\rangle_{\text{expt}}$  has been made on the basis of full-space (within  $sd$ -shells) shell-model calculations to extract a common empirical factor ( $\sim 0.78$ ) for the quenching of  $\langle\sigma\tau\rangle$ , and this value is understood<sup>13,14</sup> in terms of higher-order effects, i.e., tensor correlation, meson exchange, and  $\Delta$ -isobar excitation.<sup>15-17</sup> In the  $f_{7/2}$  shell region all the pairs of mirror nuclei ( $T = \frac{1}{2}$ ) have been found (recently, the data of  $^{51}\text{Fe}$  and  $^{55}\text{Ni}$  have been revised<sup>18</sup>), and in the  $p_{3/2}$  shell region two mirror pairs,  $^{59}\text{Zn} \rightarrow ^{59}\text{Cu}$  (Ref. 9) and  $^{57}\text{Cu} \rightarrow ^{57}\text{Ni}$ , are now available. Figure 4 summarizes the experimental  $\langle\sigma\tau\rangle$  values,  $\langle\sigma\tau\rangle_{\text{expt}}$ , for the superallowed mirror transitions in the  $f_{7/2}$ - $p_{3/2}$  shell region. In the  $d_{5/2}$ - $s_{1/2}$  shell region the value of  $\langle\sigma\tau\rangle_{\text{expt}}$  falls rapidly from  $0.85 \langle\sigma\tau\rangle_{\text{sp}}$  to  $0.4 \langle\sigma\tau\rangle_{\text{sp}}$  (except  $^{19}\text{Ne}$ ) as one goes through the

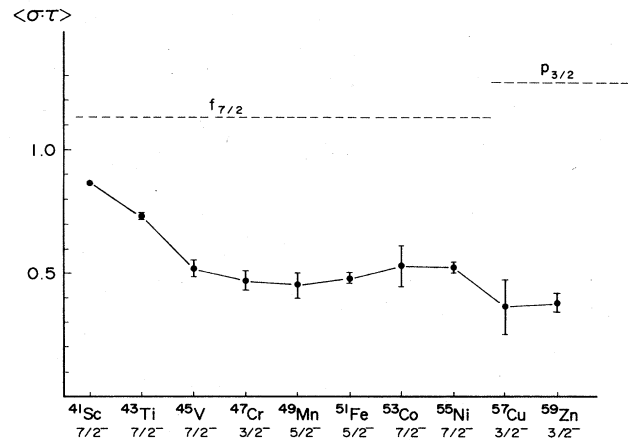


FIG. 4. Experimental  $\langle\sigma\tau\rangle$  values in the  $f_{7/2}$  and  $p_{3/2}$  shell regions,  $\langle\sigma\tau\rangle_{\text{expt}}$ , obtained using the Wilkinson's formula (Ref. 2). The masses and half-lives for calculating the  $ft$  values are taken from Refs. 4, 7, 9, and 18-23 except for  $^{57}\text{Cu}$ . The spin and parity of the ground state of the parent nucleus of a mirror transition are denoted. The dotted line indicates  $\langle\sigma\tau\rangle_{\text{sp}}$ , the extreme single-particle value of  $\langle\sigma\tau\rangle$ .

$d_{5/2}$ -shell mirror nuclei starting from  $^{17}\text{F}$ , and then  $\langle\sigma\tau\rangle_{\text{expt}}$  increases at the end of the shell ( $^{25}\text{Al}$  and  $^{27}\text{Si}$ ) and again decreases at the beginning of the  $s_{1/2}$  shell ( $^{29}\text{P}$ ). There seems to be a similar tendency, although less pronounced, in the behaviors of  $\langle\sigma\tau\rangle_{\text{expt}}$  in the  $f_{7/2}$ - $p_{3/2}$  shell region (Fig. 4), suggesting similar mechanisms of shell closure for  $\langle\sigma\tau\rangle$  in the two regions of the nuclear chart. It is, therefore, highly desirable to do systematic shell-model calculations taking into account particle-hole excitations in the  $fp$  shells (i.e.,  $f_{7/2}$ ,  $p_{3/2}$ ,  $f_{5/2}$ , and  $p_{1/2}$  shells) in order to see if there is the quenching of  $\langle\sigma\tau\rangle$  also for the  $f_{7/2}$ - $p_{3/2}$  shell region which is due to the higher-order effects.

The authors wish to thank the cyclotron crew of this Center for their assistance during this experiment. We are grateful to Professor B. H. Wildenthal and Dr. K. Ogawa for discussions, and to Professor T. Ishimatsu and Dr. E. Tanaka for their support to the present work.

<sup>1</sup>D. H. Wilkinson, Phys. Rev. C 7, 930 (1973).

<sup>2</sup>D. H. Wilkinson, Nucl. Phys. A209, 470 (1973).

<sup>3</sup>Cyclotron and Radioisotope Center Report, Tohoku University, CYRIC Annual Report, 1982, p. 54.

<sup>4</sup>Table of Isotopes, edited by C. M. Lederer and V. S. Shirley (Wiley, New York, 1978), p. 167.

<sup>5</sup>K. Takahashi, M. Yamada, and T. Kondoh, At. Data Nucl. Data Tables 12, 101 (1973).

<sup>6</sup>M. Blann, OVERLAID ALICE, Report No. COO-3494-29, 1975.

<sup>7</sup>A. H. Wapstra and K. Bos, At. Nucl. Data Tables 19, 177 (1977).

<sup>8</sup>D. M. Rehfield, R. B. Moore, and D. Hetherington, Nucl. Instrum. Methods 178, 565 (1980).

<sup>9</sup>Y. Arai, E. Tanaka, H. Miyatake, M. Yoshii, T. Ishimatsu, T. Shinozuka, and M. Fujioka, Nucl. Phys. A420, 193 (1984).

<sup>10</sup>J. Jänecke, Isospin in Nuclear Physics, edited by D. H. Wilkinson (North-Holland, Amsterdam, 1968).

<sup>11</sup>D. H. Wilkinson and B. E. F. Macefield, Nucl. Phys. A232, 58 (1974).

<sup>12</sup>A. G. M. van Hees, P. W. M. Glaudemans, and B. C. Metsch, Z. Phys. A 293, 327 (1979).

<sup>13</sup>B. A. Brown, W. Chung, and B. H. Wildenthal, Phys. Rev. Lett. 40, 1631 (1978); B. H. Wildenthal, Progress in Particle and Nuclear Physics, edited by D. H. Wilkinson (Pergamon, New York, 1983), Vol. 11, p. 5.

<sup>14</sup>B. H. Wildenthal, Proceedings of the International Symposium on Electromagnetic Properties of Atomic Nuclei, Tokyo (1983), edited by H. Horie and H. Ohnuma, p. 42; B. A. Brown and B. H. Wildenthal, Phys. Rev. C 28, 2397 (1983).

<sup>15</sup>K. Shimizu, M. Ichimura, and A. Arima, Nucl. Phys. A226, 282 (1974).

<sup>16</sup>I. S. Towner and F. C. Khanna, Nucl. Phys. A399, 334 (1983).

<sup>17</sup>M. Rho, Nucl. Phys. A354, 3c (1981).

- <sup>18</sup>J. Äystö, J. Ärje, V. Koponen, P. Taskinen, H. Hyvonen, A. Hautajarvi, and K. Vierinen, *Phys. Lett.* **138B**, 369 (1984).
- <sup>19</sup>S. Raman, C. A. Houser, T. A. Walkiewicz, and I. S. Towner, *At. Data Nucl. Data Tables* **21**, 567 (1978).
- <sup>20</sup>P. Hornshøj, J. Kolind, and N. Rud, *Phys. Lett.* **116B**, 4 (1982).
- <sup>21</sup>J. C. Hardy, H. Schmeing, E. Hagberg, W. Perry, J. Wills, E. T. H. Clifford, V. Koslowsky, I. S. Towner, J. Camplan, B. Rosenbaum, R. Kirchner, and H. Evans, *Phys. Lett.* **91B**, 207 (1980).
- <sup>22</sup>D. Müller, E. Kashy, W. Benenson, and H. Nann, *Phys. Rev. C* **12**, 51 (1975).
- <sup>23</sup>B. Sherrill, K. Beard, W. Benenson, B. A. Brown, E. Kashy, W. E. Ormand, H. Nann, J. J. Kehayias, A. D. Bacher, and T. E. Ward, *Phys. Rev. C* **28**, 1712 (1983).